Validation of Finite Element Crash Test Dummy Models for Predicting *Orion* Crew Member Injuries During a Simulated Vehicle Landing

Al Tabiei
University of Cincinnati, Cincinnati, Ohio

Charles Lawrence
Glenn Research Center, Cleveland, Ohio

Edwin L. Fasanella
Langley Research Center, Hampton, Virginia

NASA STI Program . . . in Profile

Since its founding, NASA has been dedicated to the advancement of aeronautics and space science. The NASA Scientific and Technical Information (STI) program plays a key part in helping NASA maintain this important role.

The NASA STI Program operates under the auspices of the Agency Chief Information Officer. It collects, organizes, provides for archiving, and disseminates NASA's STI. The NASA STI program provides access to the NASA Aeronautics and Space Database and its public interface, the NASA Technical Reports Server, thus providing one of the largest collections of aeronautical and space science STI in the world. Results are published in both non-NASA channels and by NASA in the NASA STI Report Series, which includes the following report types:

- TECHNICAL PUBLICATION. Reports of completed research or a major significant phase of research that present the results of NASA programs and include extensive data or theoretical analysis. Includes compilations of significant scientific and technical data and information deemed to be of continuing reference value. NASA counterpart of peer-reviewed formal professional papers but has less stringent limitations on manuscript length and extent of graphic presentations.

- TECHNICAL MEMORANDUM. Scientific and technical findings that are preliminary or of specialized interest, e.g., quick release reports, working papers, and bibliographies that contain minimal annotation. Does not contain extensive analysis.

- CONTRACTOR REPORT. Scientific and technical findings by NASA-sponsored contractors and grantees.

- CONFERENCE PUBLICATION. Collected papers from scientific and technical conferences, symposia, seminars, or other meetings sponsored or cosponsored by NASA.

- SPECIAL PUBLICATION. Scientific, technical, or historical information from NASA programs, projects, and missions, often concerned with subjects having substantial public interest.

- TECHNICAL TRANSLATION. English-language translations of foreign scientific and technical material pertinent to NASA's mission.

Specialized services also include creating custom thesauri, building customized databases, organizing and publishing research results.

For more information about the NASA STI program, see the following:

- Access the NASA STI program home page at *http://www.sti.nasa.gov*

- E-mail your question via the Internet to *help@sti.nasa.gov*

- Fax your question to the NASA STI Help Desk at 301–621–0134

- Telephone the NASA STI Help Desk at 301–621–0390

- Write to:
  NASA Center for AeroSpace Information (CASI)
  7115 Standard Drive
  Hanover, MD 21076–1320

NASA/TM—2009-215476

Validation of Finite Element Crash Test Dummy Models for Predicting *Orion* Crew Member Injuries During a Simulated Vehicle Landing

Al Tabiei
University of Cincinnati, Cincinnati, Ohio

Charles Lawrence
Glenn Research Center, Cleveland, Ohio

Edwin L. Fasanella
Langley Research Center, Hampton, Virginia

National Aeronautics and
Space Administration

Glenn Research Center
Cleveland, Ohio 44135

March 2009

Acknowledgments

The support of this work by the NASA Engineering Safety Center is greatly appreciated.

Validation of Finite Element Crash Test Dummy Models for Predicting *Orion* Crew Member Injuries During a Simulated Vehicle Landing

Al Tabiei
University of Cincinnati
Cincinnati, Ohio 45221

Charles Lawrence
National Aeronautics and Space Administration
Glenn Research Center
Cleveland, Ohio 44135

Edwin L. Fasanella
National Aeronautics and Space Administration
Langley Research Center
Hampton, Virginia 23681

Summary

A series of crash tests were conducted with dummies during simulated *Orion* crew module landings at the Wright-Patterson Air Force Base. These tests consisted of several crew configurations with and without astronaut suits. Some test results were collected and are presented. In addition, finite element models of the tests were developed and are presented. The finite element models were validated using the experimental data, and the test responses were compared with the computed results. Occupant crash data, such as forces, moments, and accelerations, were collected from the simulations and compared with injury criteria to assess occupant survivability and injury. Some of the injury criteria published in the literature is summarized for completeness. These criteria were used to determine potential injury during crew impact events.

Introduction

During the landing of the *Orion* crew vehicle on hard surfaces, significant impulse loads could be transmitted to the astronauts through the vehicle-occupant interfaces such as the floor and seat. If these loads are not attenuated to survivable levels, they could lead to severe injuries or fatality of the occupants. Simple seat structures are not sufficient to protect an occupant against hard landing; thus, further protective techniques need to be investigated.

Tabiei and Nilakantan (2007) present several concepts for impulse mitigation during a high-acceleration event. One such concept is an Energy Absorbing Seat Mechanism that cushions an occupant against shock impulses by absorbing the kinetic energy of the landing and attenuating acceleration impulses transmitted to the occupant to survivable levels.

Concepts that are used in the crashworthiness analysis of aircraft seats may be quite similar to those that will be used in crew protection during the *Orion* landing. In 1988, Fox performed a feasibility study for an OH–58 helicopter energy-attenuating crew seat. Energy-attenuating concepts included a pivoting seat pan, a guided bucket, and a tension seat. In 1989, Simula, Inc., prepared an Aircraft Crash Survival Design Guide (Desjardins et al., 1989) for the U.S. Army Aviation Applied Technology Directorate. The guide outlined various injury criteria, energy-absorbing devices, and related topics. In 1990, Gowdy (1990) designed a crashworthy seat for commuter aircraft using a wire-bending energy-absorber design.

This design was suboptimal, but it provided satisfactory results for vertical decelerations between 15g and 32g. In 1993, Laananen used Seat/Occupant Model—Light Aircraft (SOM–LA) to analyze the crashworthiness of commuter aircraft seats during full-scale impact. He concluded that the designs did not meet the 1993 standards for occupant safety and that vertical-direction energy-absorbing devices needed to be implemented. In 1994, Haley and Palmer evaluated a retrofit OH–58 pilot's seat to study its effectiveness in preventing back injury. In 1996, Alem and Strawn evaluated an energy-absorbing truck seat to evaluate its effectiveness in protection against landmine blasts. In 2002, Kellas and Jones designed an energy-absorbing seat for an agricultural aircraft using the axial crushing of aluminum tubes as the primary energy absorber. Kecman (1997) briefly summarized the approach adopted during the design of vehicle crashworthy structures that utilize joints and thin-walled beams.

The present study focused on the development of finite element (FE) occupant models and FE analysis of simulated landing events during the *Orion* landing. Simulations were conducted using the large-scale simulation code LS–DYNA (2007). A numerical version of the 50th-percentile HYBRID III Anthropomorphic Test Device (ATD) (or test dummy) was used to simulate the human occupant. Data such as head, chest, and torso acceleration, and dummy-structure contact forces were collected during the simulation and analyzed for injury assessment.

Test data were used to validate the FE model so that the effectiveness of the FE models in replicating the physical crash test dummy response during tests could be determined. A set of experiments was conducted at the Wright-Patterson Air Force Base (WPAFB) in Dayton, Ohio. Computed crash test dummy responses such as forces, moments, and accelerations were compared with test data and injury criteria to assess occupant survivability and human injury.

Review of Human Injury Tolerance Criteria

Injury criteria need to be defined in order to determine the effectiveness of a design to protect occupants from injury during crashes and hard landings. Occupant crash data such as forces, moments, and accelerations were collected from simulations and then compared with these injury criteria to assess occupant survivability and human injury. Some of the injury criteria published in the literature is summarized herein for completeness (Tabiei and Nilakantan, 2007, and Schmitt et al., 2004). It is important to note that the injury criteria presented in this work are primarily applicable to automotive safety; they are not directly applicable to space applications such as the *Orion* crew exploration vehicle since *Orion* requirements and allowable probability and severity of injuries are different from what is used for automotive safety. Automotive safety criteria and the extensive study that has gone into the criteria will be extremely useful for developing the *Orion* crew safety criteria for landings; however, additional study will be required before the automotive injury criteria can be used for the *Orion* program. In the present study, the dummy response was assessed against current automotive injury standards. Future studies are planned to assess injuries using *Orion*-specific injury standards as these standards become available.

Generalized Human Tolerance Limits to Acceleration

Table I displays the human tolerance limits for a well-restrained young male for typical crash impulses along three mutually orthogonal axes. These values provide a general outline of the safe acceleration limit for a human during a typical crash. Biological data obtained from human test subjects indicates that higher acceleration impulses can be sustained for shorter durations and that lower acceleration impulses can be sustained for longer durations. This indicates that the duration of the acceleration is important; however, Table I does not specify the time duration of the applied acceleration impulse.

TABLE I.—HUMAN TOLERANCE LIMITS
TO ACCELERATION

Occupant's direction of accelerative force (coordinate direction)	Occupant's inertial response	Tolerance level, g
Headward (x)	Eyeballs down	25
Tailward (x)	Eyeballs up	−15
Lateral right (y)	Eyeballs left	20
Lateral left (y)	Eyeballs right	−20
Back to chest (z)	Eyeballs in	45
Chest to back (z)	Eyeballs out	−45

Injury Scaling

Injury scaling is a technique for assigning a numerical assessment or severity score to traumatic injuries. The most extensively used injury scale is the Abbreviated Injury Scale (AIS) developed by the American Association for Automotive Medicine, which was originally published in 1971. The AIS assigns an injury severity of 1 to 6 to different anatomical injuries. Table II provides the AIS designations and gives examples of head and spine injuries. The primary limitation of the AIS is that it looks at each injury in isolation and does not indicate the probable outcome for the whole individual. Consequently, the Injury Severity Score (ISS) was developed in 1974 to predict probability of survival. The ISS is derived by summing the squares of the three regions of the body with the highest AIS values. This gives an ISS ranging from 1 to 75. The maximal value of 75 would result from three AIS–5 injuries or one or more AIS–6 injuries. Probabilities of death have been assigned to each possible score.

TABLE II.—ABBREVIATED INJURY SCALE (AIS) SCORES AND
SAMPLE INJURY TYPES FOR TWO BODY REGIONS

AIS	Severity	Head	Spine
0	None	------------------------------------	----------------------------------
1	Minor	Headache or dizziness	Acute strain (no fracture or dislocation)
2	Moderate	Unconsciousness less than 1 hr; linear fracture	Minor fracture without any cord involvement
3	Serious	Unconscious 1 to 6 hr; depressed fracture	Ruptured disc with nerve root damage
4	Severe	Unconscious 6 to 24 hr; open fracture	Incomplete cervical cord syndrome
5	Critical	Unconscious more than 24 hr; large hematoma	C4 or below cervical complete cord syndrome
6	Maximum injury (virtually nonsurvivable)	Crush of skull	C3 or above cervical complete cord syndrome

Dynamic Response Index

The Dynamic Response Index (DRI) represents the maximum dynamic compression of the vertebral column and is calculated by describing the human body in terms of an analogous, lumped-mass-parameter mechanical model consisting of a mass, spring, and damper (Brinkley et al., 1989). The DRI model assesses the response of the human body to transient acceleration-time profiles. The DRI has been effective in predicting potential spinal injury for positive z-acceleration environments in ejection seats. DRI is acceptable for evaluating crash-resistant seat performance relative to spinal injury if it is used in conjunction with other injury criteria including Eiband and lumbar-load thresholds (Brinkley et al., 1989). Acceleration limits for the DRI are provided in Table III.

TABLE III.—DYNAMIC RESPONSE (DR) LIMITS FROM BRINKLEY ET AL. (1989)

DR level	Acceleration direction (occupant's inertial response)					
	x (eyeballs out, in)		y (eyeballs right, left)		z (eyeballs up, down)	
	$DR_x < 0$	$DR_x > 0$	$DR_y < 0$	$DR_y > 0$	$DR_z < 0$	$DR_z > 0$
Low[a]	−28	35	−14	14	−13.4	15.2
Moderate	−35	40	−17	17	−16.5	18
High risk	−46	46	−22	22	−20.4	22.4

[a]Same as NASA specification.

Lumbar-Load Criterion

The lumbar-load criterion states that maximum compressive load shall not exceed 1500 lb (6672 N) measured between the pelvis and lumbar spine of a 50th-percentile test dummy for a crash impulse in which the predominant impact vector is parallel to the vertical axis of the spinal column. Also, the compressive load must not exceed 3800 N in a 30-ms interval. This is one of the most widely used criteria in vertical crash and impact testing. If the spinal cord is severely compressed or severed, it can lead to instant paralysis or fatality (Fox, 1988; Kellas and Jones, 2002; Schmitt et al., 2004; and Brinkley et al., 1989).

Head Injury Criterion

The Head Injury Criterion (HIC) was proposed by the National Highway Traffic Safety Administration (NHTSA) in 1972 and is an alternative interpretation to the Wayne State Tolerance Curve. It is used to assess forehead impact against unyielding surfaces. Basically, the acceleration-time response is experimentally measured, and the data are related to skull fractures.

Gadd (1966) had suggested a weighted-impulse criterion (Gadd Severity Index, GSI) as an evaluator of injury potential. He used a log scale and an approximate straight line function to plot the Wayne State Tolerance Curve data for the weighted impulse criterion that eventually became known as the GSI:

$$\text{GSI} = \int_t a^n dt \qquad (1)$$

where

a acceleration as a function of time
n weighting factor greater than 1
t time

The HIC is given by

$$\text{HIC} = (t_2 - t_1)\left[\int_{t_2}^{t_1} a(t)dt\right]^{2.5} \qquad (2)$$

where

$a(t)$ acceleration as a function of time of the head center of gravity

t_1, t_2 time limits of integration that maximize HIC

Federal Motor Vehicle Safety Standard (FMVSS) 208 originally set a maximum value of 1000 for the HIC and specified a time interval not exceeding 36 ms (or HIC_{36}). If the HIC is 1000, there is a 16-percent probability of a life-threatening brain injury. The HIC suggests that a higher acceleration for a shorter period is less injurious than a lower level of acceleration for a longer period. As of 2000, the NHTSA final rule specified the maximum acceleration time for calculating the HIC as 15 ms (or HIC_{15}; see Gowdy, 1990; Gadd, 1966; Tyrell and Severson, 1996; Armenia-Cope et al., 1993; Kleinberger et al., 1999; McHenry, 2004; and Nirula et al., 2003). Table IV shows the HIC for various dummy sizes.

TABLE IV.—HEAD INJURY
CRITERION (HIC) FOR VARIOUS
DUMMY SIZES

Dummy type	HIC_{15} limit[a]
Large male	700
Mid-size male	700
Small female	700
6-year-old child	700
3-year-old child	570
1-year-old infant	390

[a]For maximum acceleration time of 15 ms.

Head Impact Power

A 2004 report (Schmitt et al.) proposed a new HIC entitled Head Impact Power. This criterion considers not only kinematics of the head (rigid body motion of the skull) but also the change in the kinetic energy of the skull, which may deform and injure nonrigid brain matter. Head Impact Power is based on the general rate of change of the translational and rotational kinetic energy. It is an extension of the Viscous Criterion first proposed by Lau and Viano in 1986, which states that a certain level or probability of injury will occur to a viscous organ if the product of its compression C and the rate of compression V exceed some limiting value.

Injury Assessment Reference Values

The injury assessment reference values adopt new requirements for specifications, instrumentation, test procedures, and calibration for the Hybrid III test dummy (Kecman, 1997). The regulation's preamble has a detailed discussion of the injury mechanisms and the relevant automotive mishap data for each of the injury criteria associated with the Hybrid III dummy. Military test plans should implement these criteria.

Neck Injury Criteria

The Neck Injury Criteria (NIC) considers relative acceleration between the first cervical (C1) and first thoracic (T1) vertebra (Teng et al., 2004, Nusholtz, G.S., et al. (2003)) and is given by

$$\mathrm{NIC}(t) = 0.2 x a_{\mathrm{rel}}(t) + \left[v_{\mathrm{rel}}(t) \right]^2 \tag{3}$$

where

$$a_{\mathrm{rel}}(t) = a_x^{\mathrm{head}}(t) \quad \text{and} \quad v_{\mathrm{rel}}(t) = \int a_x^{T1}(t) - \int a_x^{\mathrm{head}}(t) \tag{4}$$

NIC must not exceed 15 m^2/s^2 (Welcher and Szabo, 2001). Another criteria, NIC_{50}, refers to NIC at 50 mm of C1–T1 (cervical-thoracic) retraction.

The N_{ij} criteria proposed by NHTSA combine the effects of forces and moments measured at the occipital condyle and are a better predictor of craniocervical injuries. The N_{ij} criteria take into account N_{TE} (tension-extension), N_{TF} (tension-flexion), N_{CE} (compression-extension), and N_{CF} (compression-flexion). FMVSS 208 requires that none of the four N_{ij} values exceed 1.4 at any point. The generalized N_{ij} (Croft et al., 2002) is given by

$$N_{ij} = \left(\frac{F_z}{F_{zc}}\right) + \left(\frac{M_y}{M_{yc}}\right)$$

(5)

where

F_z	upper neck axial force, N
M_y	moment about occipital condyle
F_{zn}	axial force critical value, N
M_{yn}	moment critical value, N-m

The FMVSS 208 (2000) final rule also uses N_{ij}. This criterion is based on the belief that the occipital condoyle-head junction can be approximated by a prismatic bar and that the failure for the neck is related to the stress in the ligament tissue spanning the area between the neck and the head. The N_{ij} criterion must not exceed 1.0 (Gadd, 1966; Nirula et al., 2003; Welcher and Szabo, 2001; and Bostroem et al., 1998).

Chest Criteria

Peak resultant acceleration must not exceed 60g for more than 3 ms (Mertz and Gadd, 1971, and Mertz and Patrick, 1971) as measured by a triaxial accelerometer in the upper thorax. Also, the chest compression must be less than 3 in. for the Hybrid III dummy as measured by a chest potentiometer behind the sternum.

Viscous Criterion

The Viscous Criterion is defined as the chest compression velocity (derived by differentiating the measured chest compression) multiplied by the chest compression and divided by the chest depth. This criterion is mentioned for the sake of completeness; it is not widely used (Schmitt et al., 2004).

Femur Force Criterion

The femur force criterion states that the compressive force transmitted axially through each upper leg should not exceed a certain value. Impulse loads that exceed this limit can cause complete fracture of the femoral bone as well as sever major arteries that can cause excessive bleeding. Different references state different values for the maximum allowable compressive axial force. Wayne State University states a maximum allowable value of 10 000 N. The Department of Army states that the axial compression force shall not exceed 7562 N in a 10-ms interval and 9074 N at any instant.

In numerical dummies, discrete spring elements of known stiffness are included within the leg model, from which the femur axial compressive force is easily extracted. In actual dummies, load cells are placed on the dummy's leg, which are calibrated to provide the compressive force at the femur.

Thoracic Trauma Index

The thoracic trauma index (TTI) is given by

$$\text{TTI}(d) = \frac{1}{2}\left(G_R + G_{LS}\right) \tag{6}$$

where

G_R greater of the peak accelerations of either the upper or lower rib, g
G_{LS} lower spine peak acceleration, g

The pelvic acceleration must not exceed 130g (Schmitt et al., 2004).

Combined Thoracic Index

The combined thoracic index considers both the chest defection and chest acceleration. For a 50th-percentile male dummy, the chest acceleration should not exceed 60g for a 3-ms impulse. The chest deflection should not exceed 63 mm.

Finite Element Dummy Model

The Hybrid III FE dummy used in this work was developed and validated by Livermore Software Technology Corporation (LSTC). A full set of LSTC Hybrid III FE dummies were modeled in LS–DYNA format and set up according to the Society of Automotive Engineering (SAE) calibration procedures for Hybrid III test dummies. The FE dummy used herein was modeled using rigid and deformable parts. This dummy was validated by LSTC using standard impact tests in four different locations and positions as shown in Figures 1 to 5. These tests consisted of head impact (Fig. 1), neck flexion and extension (Figs. 3 and 4), chest impact (Fig. 2), and knee impact (Fig. 5). These particular tests were selected because this dummy model was validated for car crashes. However, this dummy was not validated for impacts in all possible orientations. The LSTC Hybrid III FE dummy model can be used free of charge, which makes it a good starting point for obtaining initial results for any possible impact situation involving occupant protection.

The FE dummy was imported into the preprocessor LSPREPORT to orient it in the desired position. The position had to match the position of the test dummy. This was achieved by several operations of what is called H-point translation and rotation. In addition, limb operations were available to properly position the arms and legs. The neck, however, was in a standard position that could not be altered. In the new dummy models that are being developed by LSTC, the neck can be rotated to better match the test setup; however, this model has not been validated completely. Since the validated FE neck model cannot be positioned arbitrarily, for the model to be entirely consistent with the test it is necessary to position the test dummy's neck to match the FE model.

Seat belts also were modeled with the preprocessor LSPREPORT. The FE dummy was imported into the preprocessor; then "segment sets" were defined on the FE dummy where the seat belts were to be positioned. Once these sets were defined, the seat belts were positioned on the set and tensioned to make them fit to the contour of the dummy where they contacted it. The belts can be modeled with seat belt elements (beamlike elements) or by shell elements. The shell model, however, is the most appropriate model for capturing the seat belt/dummy interaction. The pretension in the seat belt is modeled by defining a local coordinate system on the belt ends. A load is then defined in this coordinate system with a magnitude equal to the preload applied in the test setup. The load, however, must be ramped to the full magnitude. Applying full-magnitude tension at time zero can lead to unrealistic oscillations in the system response and to inaccurate simulation results.
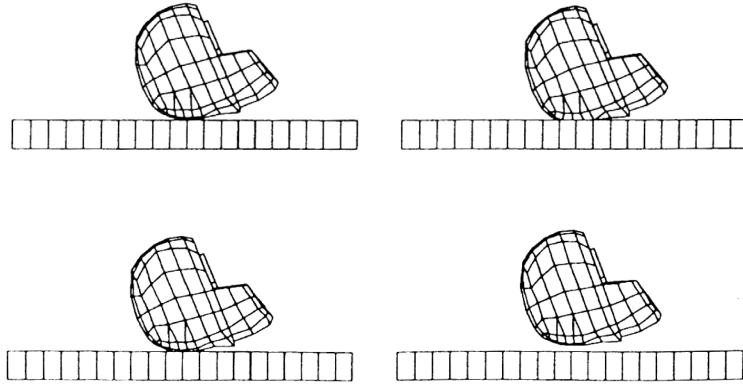
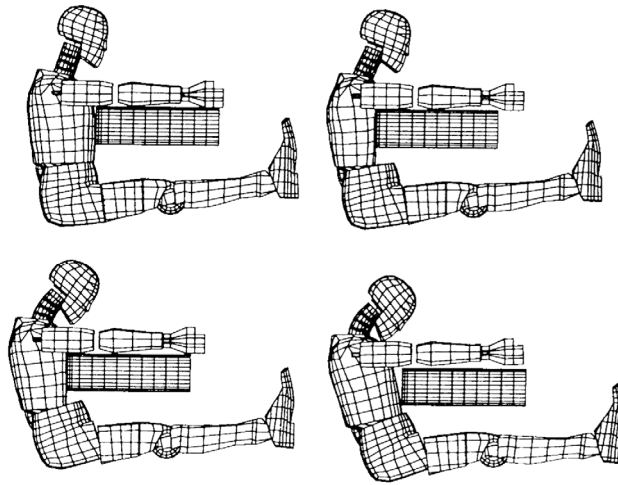Figure 1.—Head model used for test calibration.
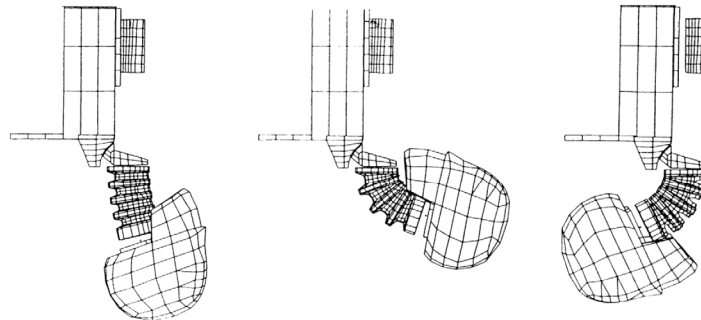

Figure 2.—Calibration test for chest impact.

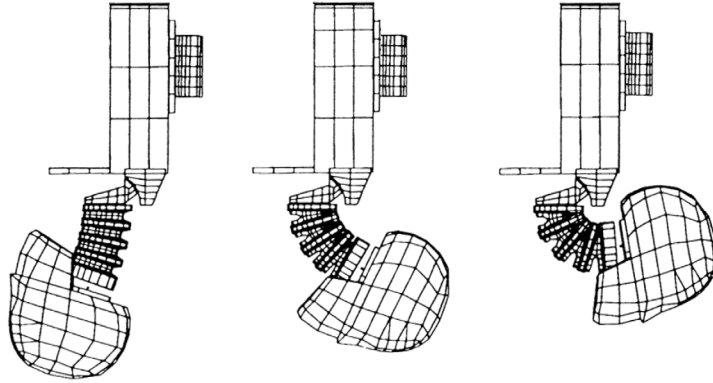Figure 3.—Calibration test for neck flexion.

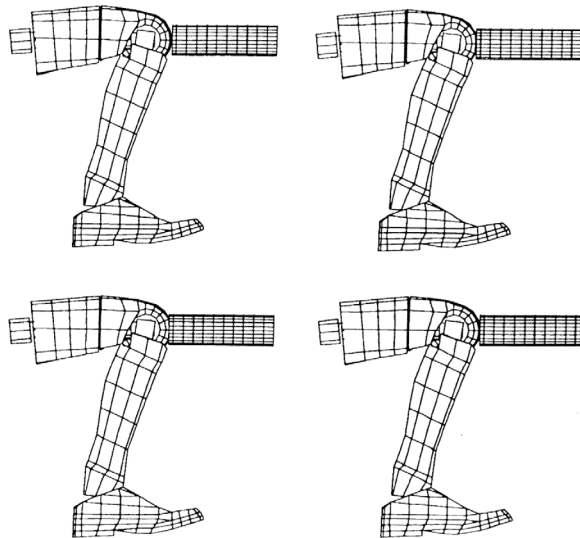Figure 4.—Calibration test for neck extension.

Figure 5.—Calibration test for knee impact.

Hybrid III Dummy Tests

Several sets of experiments were conducted at WPAFB. These tests consisted of a belted Hybrid III dummy in several configurations and various impulses (see Figs. 6 and 7). The dummy was clothed in a proposed astronaut suit and tested in several configurations as shown in Figure 8. In this paper, only two sets of tests were considered for validation and data extraction—a 10g impulse in the positive x-direction (Fig. 6) and a 20g impulse in the positive z-direction (Fig. 7). The testing at WPAFB was planned and performed primarily to assess the testing capabilities of the facility and the applicability of using the facility to test *Orion* crew seats, suits, harnesses, and protection systems. Validation of the FE dummy was not part of the original test plan; therefore, the testing was not designed to address the specific needs of the FE validation.
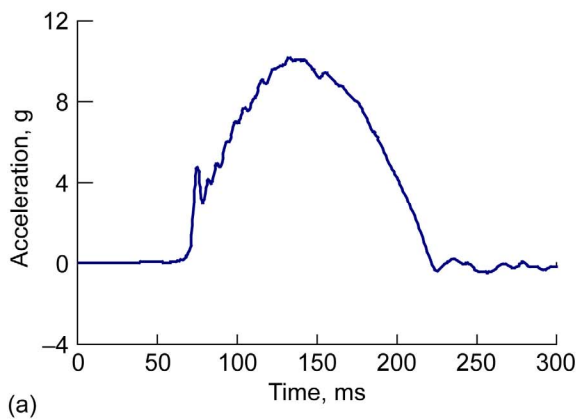
Figure 6.—Sled test with a 10g impulse in the *x*-direction. Sled motion is to the right. (a) Results. (b) Dummy position.
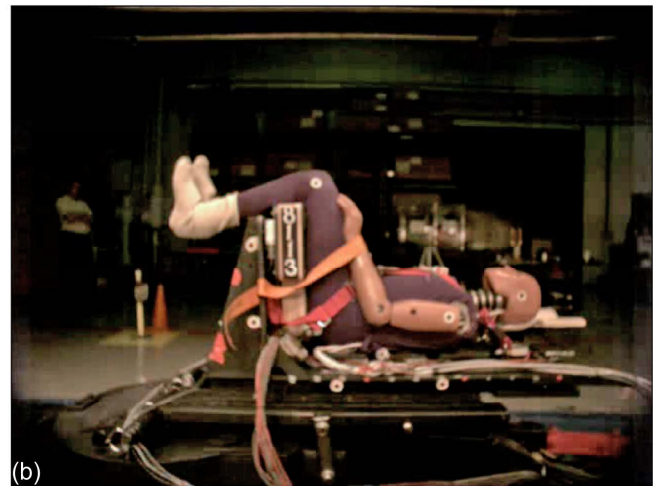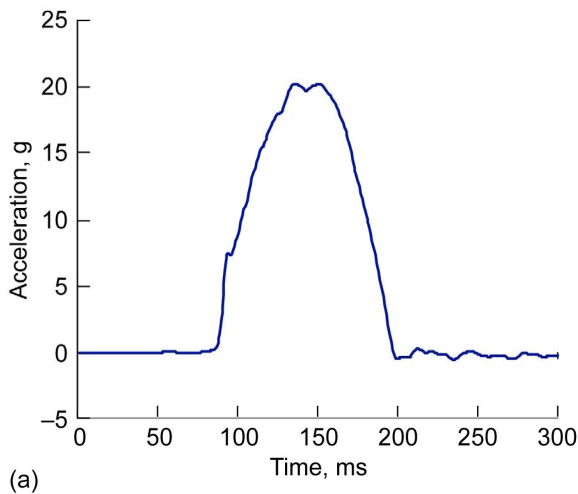
Figure 7.—Sled test with a 20g impulse in the *z*-direction. Sled motion is to the right. (a) Results. (b) Dummy position.

Figure 8.—Hybrid III dummy wearing a proposed astronaut suit.

The FE model of the Hybrid III dummy was positioned as closely as possible to the test setup, as shown in Figure 9. However, as previously mentioned, because of limitations of the Hybrid III FE neck model, the FE neck was preset to the fixed location that is typically used in the automotive industry for frontal impact tests. Consequently, the neck position differed a few degrees from the test dummy setup. This difference in neck positioning affected the forces and moments in the neck and the timing of the impact of the head with the pad located behind the head. The effect was not only in the magnitude of these forces and moments, but also in the phase. The impact between the head and the pads occurred earlier for the FE dummy than for the test dummy because of the placement of the pads between the seat and head. Since the WPAFB testing was performed before the limitation in the FE neck model was identified, there was no way to rectify the discrepancy in the neck positions. However, for future testing it would be beneficial to include any constraints in the FE dummy as part of the test plan. The pad between the dummy head and the seat also resulted in uncertainties because the actual pad thickness and material characteristics were unknown. In the simulation, assumptions were made to best fit the head data reported from the experimental testing.
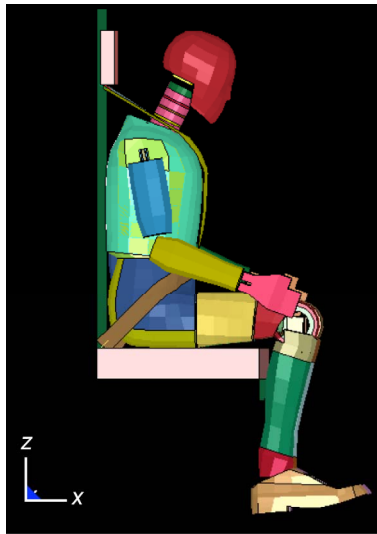
Figure 9.—Finite element dummy.

The positions of the arms and legs, as shown in Figures 9 and 10, were different for the FE dummy and test dummy. However, we concluded from several simulations that these limbs had very little effect on the kinematics of the chest, head, and pelvis. In addition, the limbs did not have any significant effects on the forces and moments collected at various locations on the dummy in the simulation.

The simulation was conducted to match the test setup as closely as possible. However, because of a mismatch between the neck and head position of the test dummy and FE dummy, some discrepancies between the predictions were possible and expected.

Simulation Validation for a 10g Impulse in the Positive *x*-Direction

The belted dummy was simulated with LS–DYNA version 971 on a personal computer using Microsoft Windows XP. The 300-ms simulations took several hours to conduct. A duration of 300 ms was selected because there was no further significant response of the dummy to the applied impulse beyond this time. Movie-editing software was used to extract a sequence of photos from the movie of the tests (WPAFB test 8088). Unfortunately, the tests and simulations could not be synchronized, so matching of the movie photos and the simulations could only be approximated. The researchers attempted to extract images from the simulations that would match the timing of the movie photos as closely as possible (Fig. 10).

The input impulse (shown in Fig. 6) was a near triangular impulse of 10g in the positive *x*-direction. This direction is equivalent to loading from a rear impact. Nominal *Orion* landings will impose a combination of rear (+*x*) and spinal (+*z*) impact loadings. The test impulse was given to the entire seat assembly because the seat was firmly attached to a relatively rigid sled that was pushed down a horizontal track by a hydraulic jack. A wooden block was set between the seat pan and the test dummy bottom in the test setup. A similar material was placed between the FE dummy bottom and FE seat. Because the FE seat was assumed to be rigid, it was modeled with rigid shell elements. The seat was given an *x*-acceleration identical to that measured for the sled because it was assumed that the seat and sled would move together as a single rigid unit. The FE model did not include the seat-sled assembly, and consequently, the proper boundary conditions on the seat are in question since it is not completely clear how the actual sled accelerations transfer to the seat. Two boundary conditions were considered in the simulation to assess the effect of boundary conditions. For the first boundary condition, the seat was assumed to be free to move freely in the *y* (sideways) and *z* (dummy spinal) directions. For the second boundary condition, the seat was only allowed to move in the impulse direction, and the *y*- and *z*-direction displacements were fully constrained. These boundary conditions predicted nearly identical results.
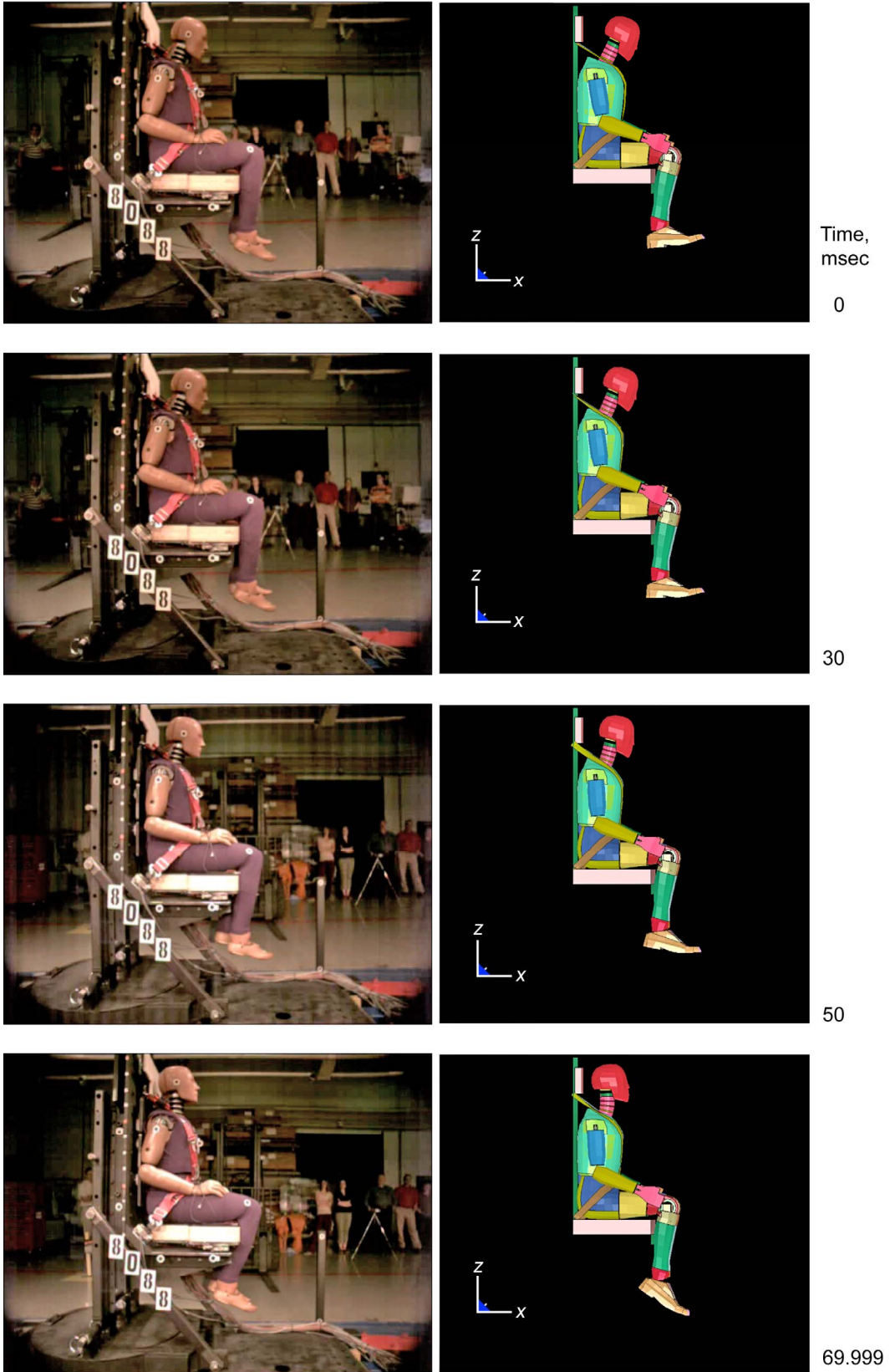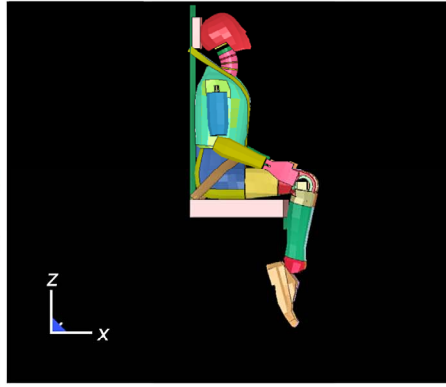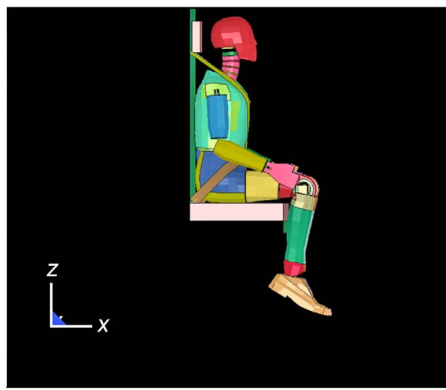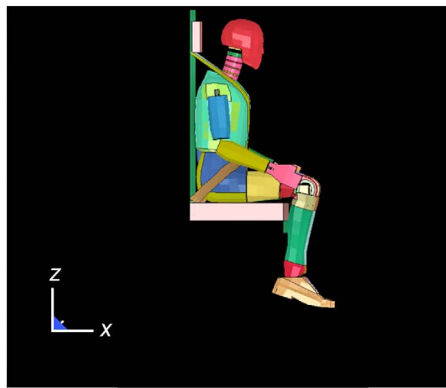
Figure 10.—Sled test with a 10g impulse in the x-direction. Sled motion is to the right in figure.
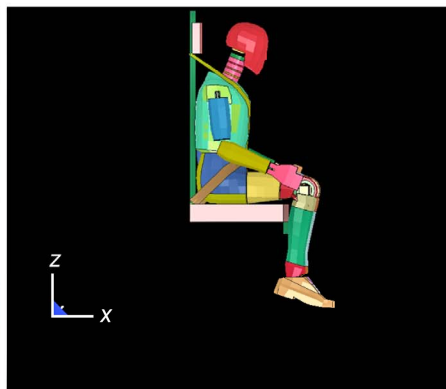
Time, msec

89.999

140

180

200

Figure 10.—Concluded.

Kinematics, force, and moment data from the simulations were collected at high frequency to include most of the responses. The corresponding data from the tests were collected at 1-ms intervals. Figure 11 presents the resultant acceleration of the dummy head from the tests and simulations. Simulation data that were filtered with a low-bypass (SAE) filter at 180 Hz are also shown in Figure 11. The magnitudes of the impulses from the simulations and tests are very close to each other. However, one can observe that there are two peaks in the test results. This is not clearly understood. The test results indicate that the test dummy's head impacted the pads on the seat twice. Movie footage confirmed this double impact. Double impact only is possible if there is a slip between the head and the pads. In the FE model, the pads were modeled with crushable foam, and only one impact between the foam and the dummy head was predicted. Overall, the magnitudes of the head accelerations for the tests and simulations were reasonably close.

Chest accelerations were extracted from the simulations and are compared with those of the test dummy in Figure 12. The simulation data and test data were filtered with the same filter and cutoff frequency (180 Hz). Here also, the experimental data are in question. If the dummy was belted as reported and a tension was applied to the belts that securely hold the test dummy to the seat, then the dummy chest should have moved with the seat and sled, and the acceleration should have matched the input impulse. However, a slip between the dummy and the seat belts would have created an additional impact force on the dummy chest and caused a higher acceleration. The chest acceleration predictions for the FE dummy were similar to the input impulse, as anticipated, since the FE dummy was constrained to move with the seat and sled.
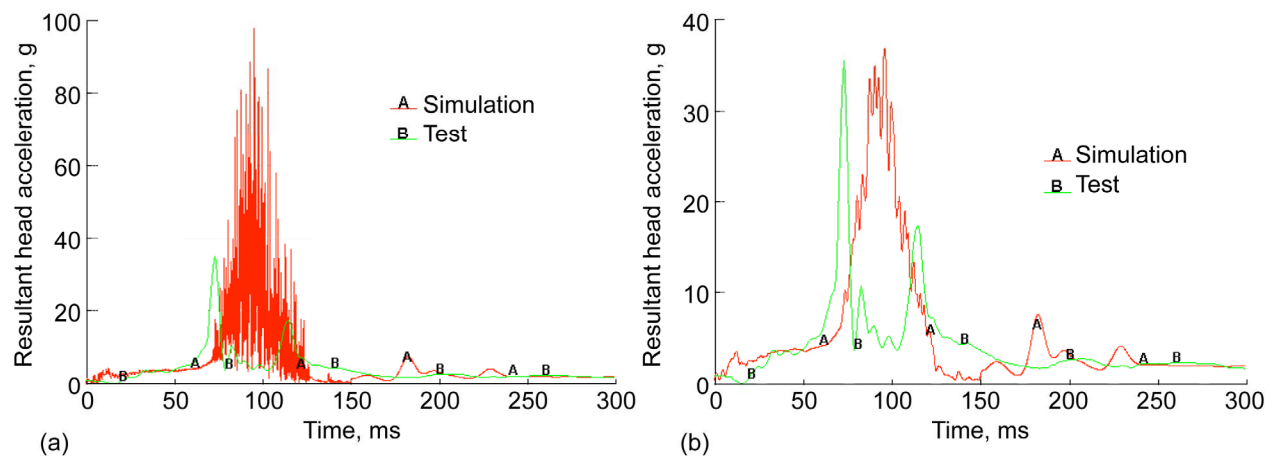

Figure 11.—Head acceleration of Hybrid III physical and finite element dummies. (a) Unfiltered. (b) Filtered at 180 Hz.
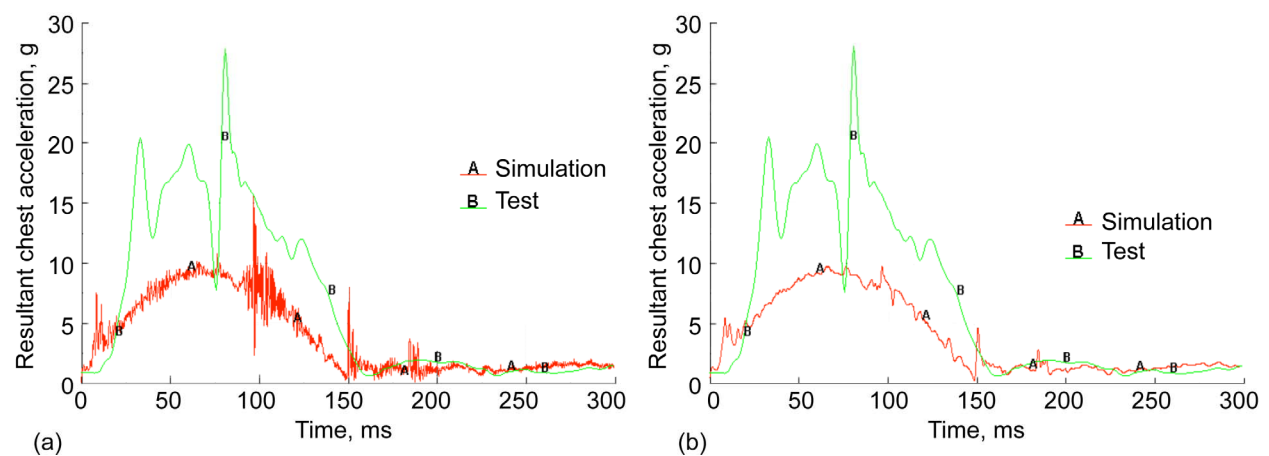

Figure 12.—Chest acceleration of Hybrid III physical and finite element dummies. (a) Unfiltered. (b) Filtered at 180 Hz.

Figure 13 shows the pelvis accelerations from the tests and simulations. Here, a much better prediction was obtained, and the pelvis accelerations of the FE dummy matched those of the test dummy very well.

For several reasons, forces and moments are normally difficult to match for FE dummies and test dummies. First, forces and moments are sensitive to the initial position of the head and neck so the position of the head and neck in the simulation has to be exactly the same as in the test, which is difficult to achieve in practice. Second, the neck and moment forces are very sensitive to any mismatch between the kinematics of the FE head and chest and the corresponding kinematics from the tests. Figure 14 depicts the neck y-moments from the tests and the simulations. As discussed earlier, one can observe the timing problem and a phase difference between the simulations and test results. In general, the experimental data yielded a higher moment than the simulation did. The test dummy head impacted the pads at about 70 ms. One can see that the neck moment was positive until the head impacted the pad; then the neck forces became negative. However, the head impacted the pads at a later time in the simulation. This explains the difference in the phase of the neck y-moment. If one shifts the simulation data in time, a better correlation is obtained.
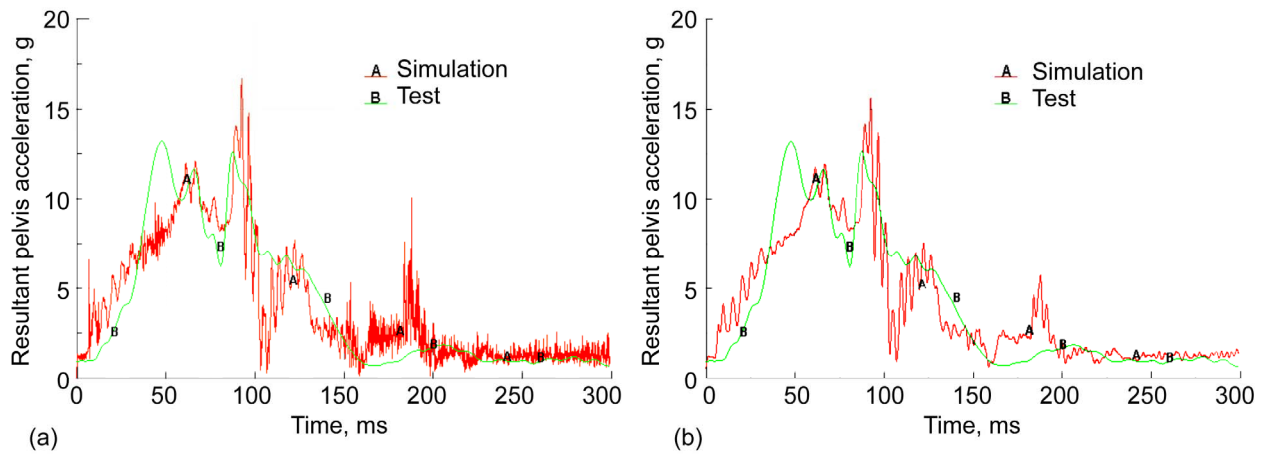

Figure 13.—Pelvis acceleration of Hybrid III physical and finite element dummies. (a) Unfiltered. (b) Filtered at 180 Hz.
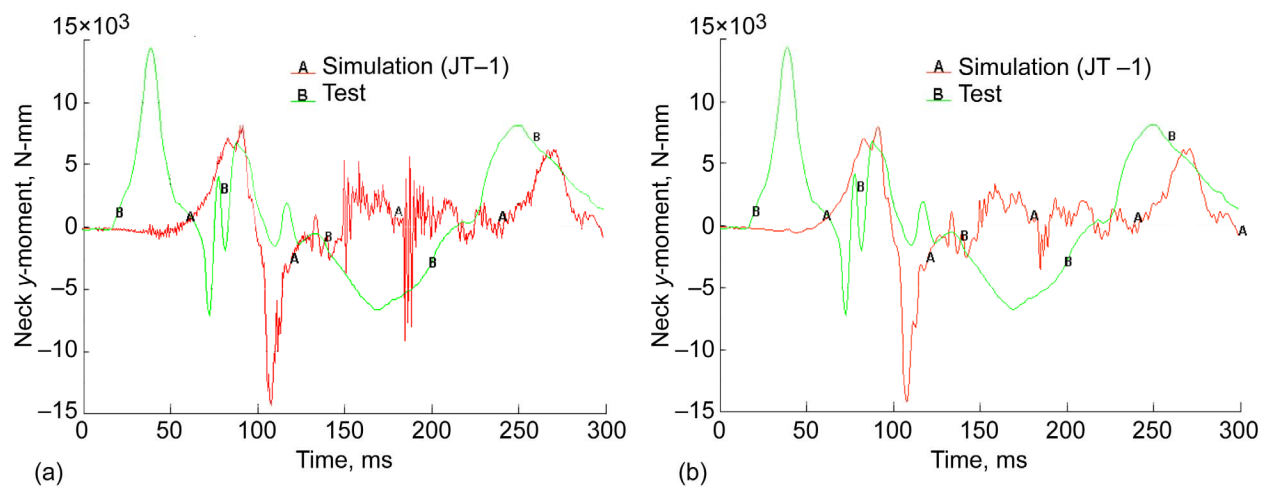

Figure 14.—Neck moment of Hybrid III physical and finite element dummies. (a) Unfiltered. (b) Filtered at 180 Hz.

Lumbar forces, which cause one of the most important injuries observed in fighter-jet ejection seats and similar events, can be extracted from the FE dummy. However, the FE dummy was not specifically designed to collect such data nor was it validated for predicting lumbar forces. The modeling of the lumbar column is relatively primitive in the Hybrid III FE dummy. To obtain accurate lumbar data, one would need to use a more elaborate FE dummy. However, the Hybrid III FE model may be useful for comparative purposes. Figure 15 shows the lumbar z-force. Lumbar forces from the test and simulation are reasonably close. The lumbar force in the x-direction also was collected and is compared with the experimental data in Figure 16. However, the correlation is not as good as for the z-forces. The figure shows a similar trend in the test and simulation.
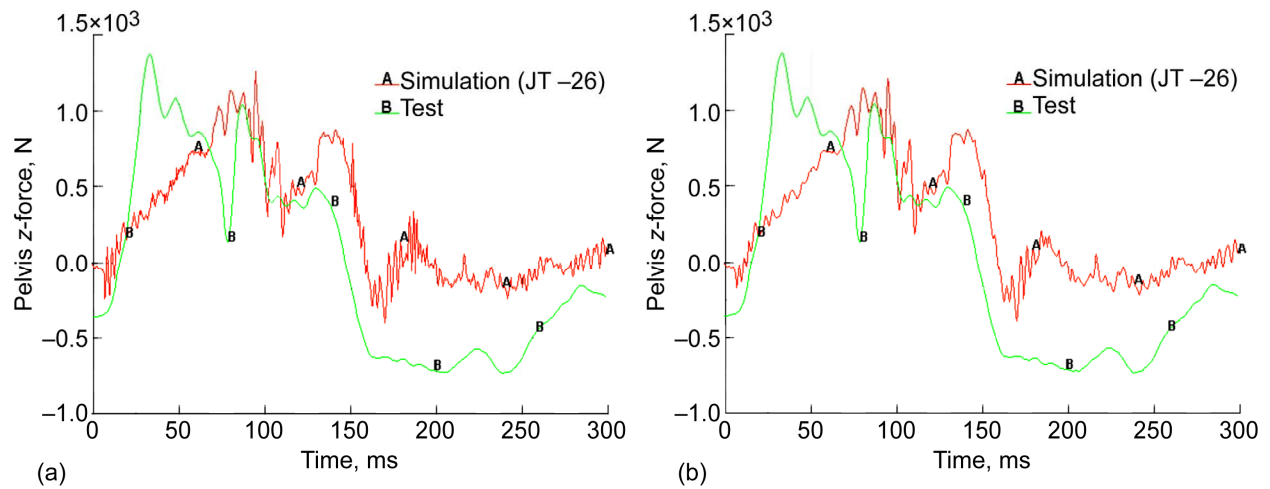

Figure 15.—Pelvis z-force of Hybrid III physical and finite element dummies. (a) Unfiltered. (b) Filtered at 180 Hz.
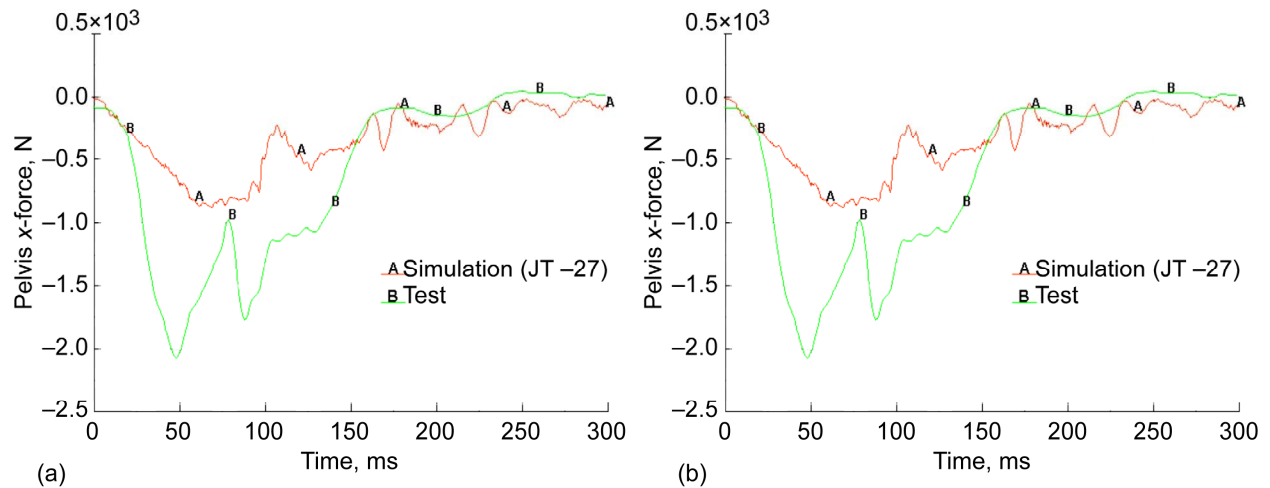

Figure 16.—Pelvis x-force of Hybrid III physical and finite element dummies. (a) Unfiltered. (b) Filtered at 180 Hz.

Simulation Validation With a 20g Impulse in the Positive *z*-Direction

As for the 10g case, the belted dummy was simulated with LS–DYNA version 971 on a personal computer using Microsoft Windows XP. Again, movie-editing software was used to extract a sequence of photos from the movie of the tests (WPAFB test 8113). Unfortunately, the tests and simulations could not be synchronized, so matching between the movie photos and the simulations could only be approximated. The researchers attempted to extract images from the simulation that would match the timing of the movie photos as closely as possible. Figure 17 shows these sequences.

The input impulse (shown in Fig. 7) was a near triangular impulse of 20g in the positive *z*-direction. This direction is equivalent to a vertical impact loading. The test impulse was given to the entire seat assembly because the seat was firmly attached to a relatively rigid sled that was pushed down a horizontal track by a hydraulic jack.

Kinematics, force, and moment data from the simulations were collected at high frequency to include most of the responses. The corresponding data from the tests were collected at 1-ms intervals. Figure 18 presents the resultant accelerations of the dummy head from the test and simulation. The magnitudes of the impulses from the simulations and tests are close to each other, but with some discrepancies. Overall, the magnitude of the head acceleration was reasonably close for the tests and simulations.

Chest accelerations were extracted from the simulation and are compared with the chest accelerations of the test dummy in Figure 19. The simulation data and test data were filtered with the same filter and cutoff frequency (180 Hz). Here also, the experimental data are in question. If the dummy was belted as reported and a tension was applied to the belts that securely hold the test dummy to the seat, then the dummy chest should have moved with the seat and sled and the acceleration should have matched the input impulse. However, a slip between the dummy and the seat belts would have created an additional impact force on the dummy chest and caused a higher acceleration. The chest acceleration predictions for the FE dummy were similar to the input impulse, as anticipated, since the FE dummy was constrained to move with the seat and sled.

Figure 20 shows the pelvis accelerations from the test and simulation. Here, a much better prediction was obtained; the pelvis accelerations of the FE dummy matched those of the test dummy very well for one of the components. However, the other component was totally off. Again, this is not well understood.

Forces and moments are the hardest parameters to match for FE dummies and test dummies. In this study, moments and forces were collected but are not presented because they do not match the test data. In general, a better prediction could be made if the test setup of the test dummy better matched the position of the FE dummy before testing was conducted. Figure 21 illustrates this point for two dummy positions and two pad thicknesses. The kinematics data are shown in Figure 22. One can observe the difference in the response due to the change of the dummy positions. Any change in the kinematics of the head would result in a greater change in the forces and moments in the neck.
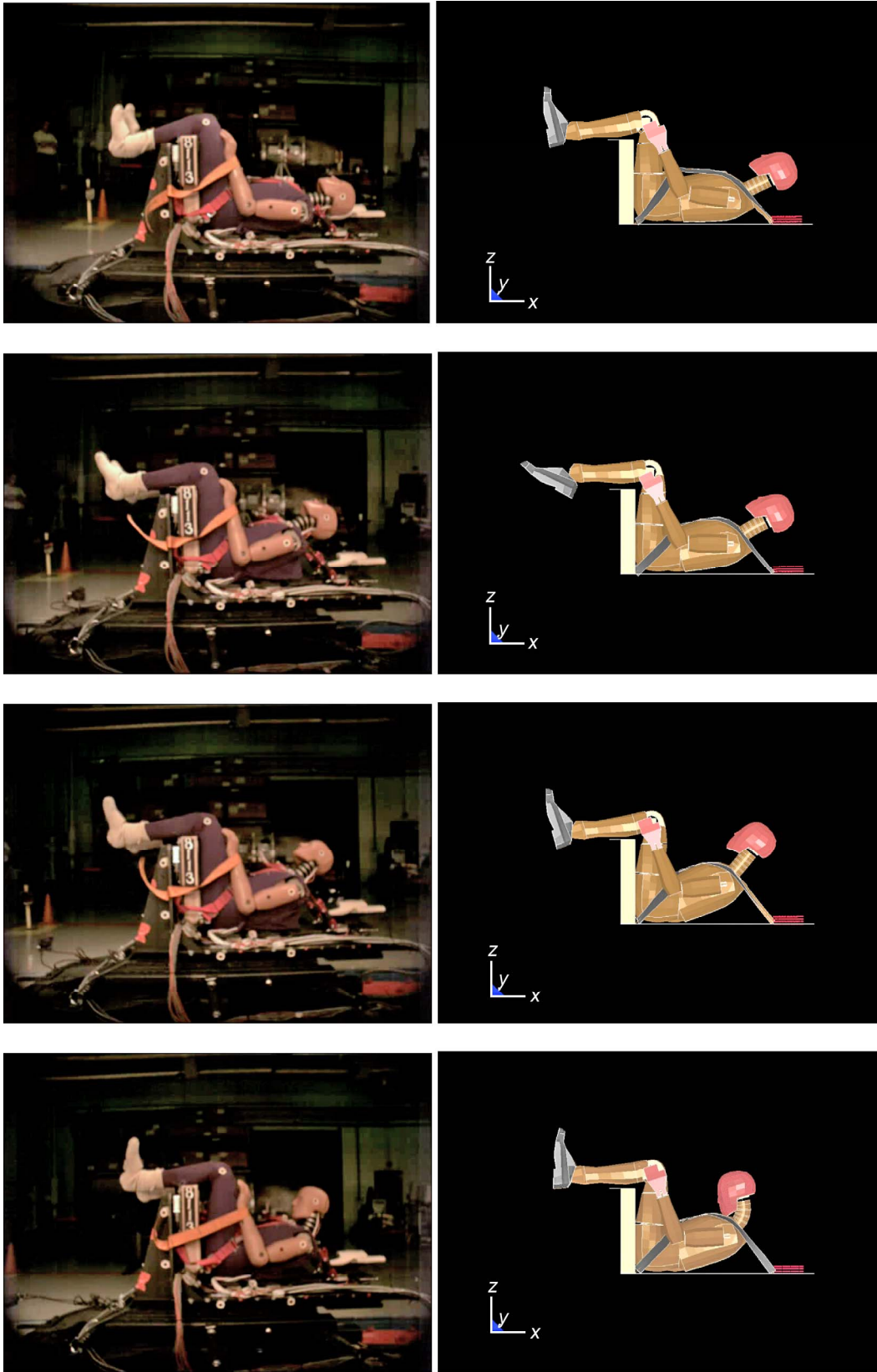
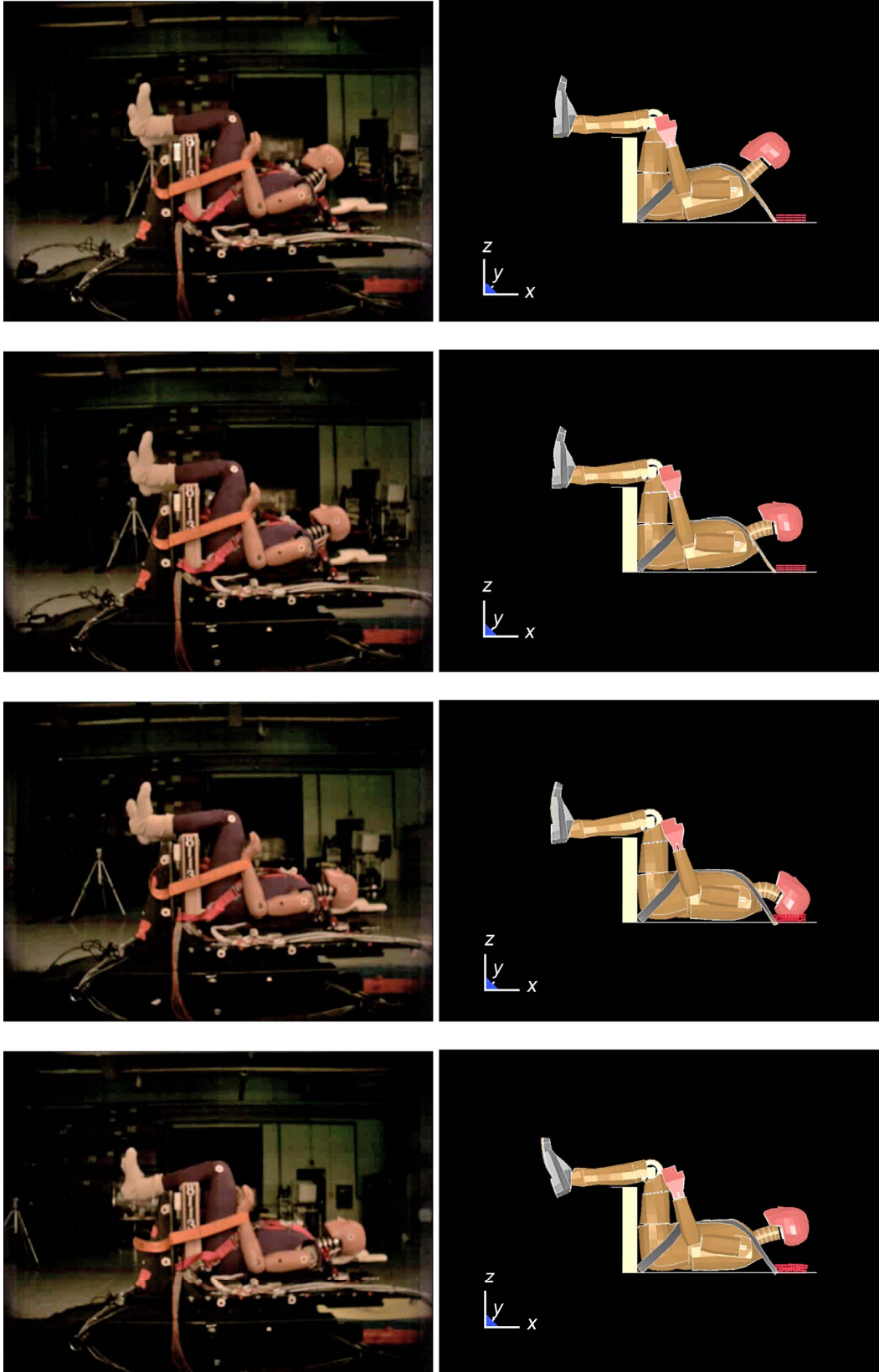Figure 17.—Sled test with a 20g impulse in the *z*-direction. Sled motion is to the right in figure.
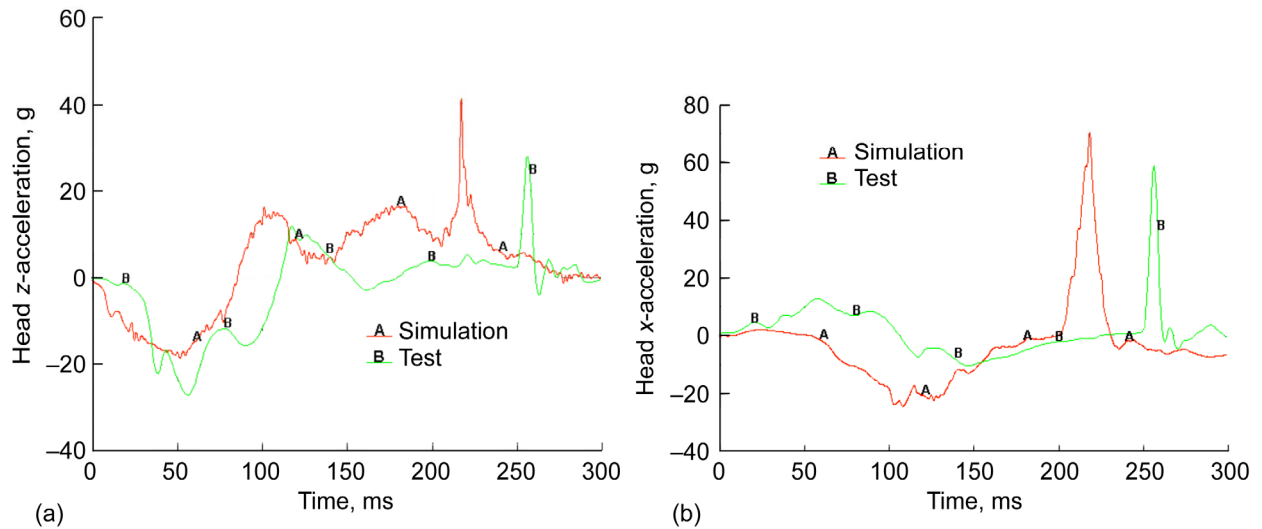
Figure 17.—Concluded.

Figure 18.—Head acceleration from Hybrid III physical and finite element dummies. (a) *z*-acceleration. (b) *x*-acceleration.
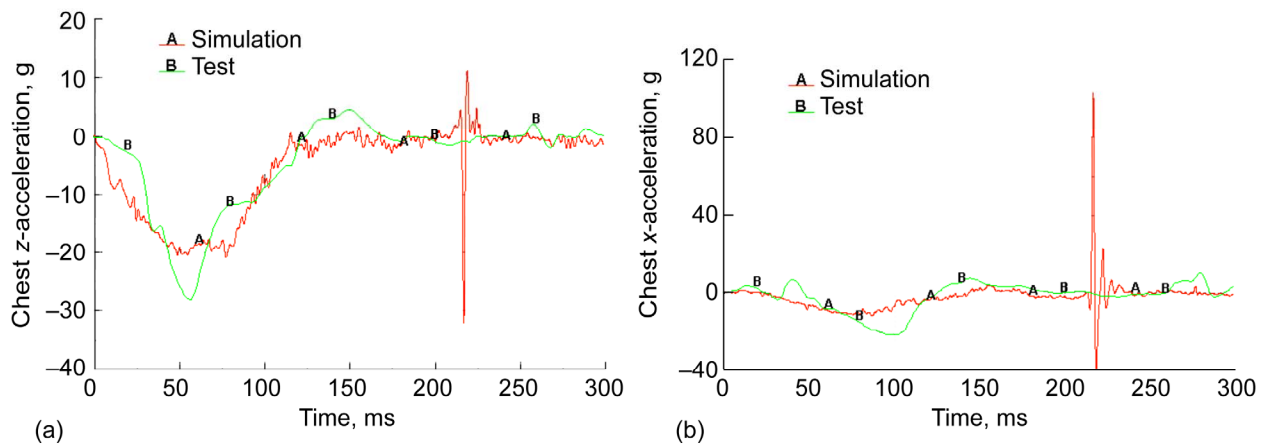

Figure 19.—Chest acceleration from Hybrid III physical and finite element dummies. (a) z-acceleration. (b) x-acceleration.
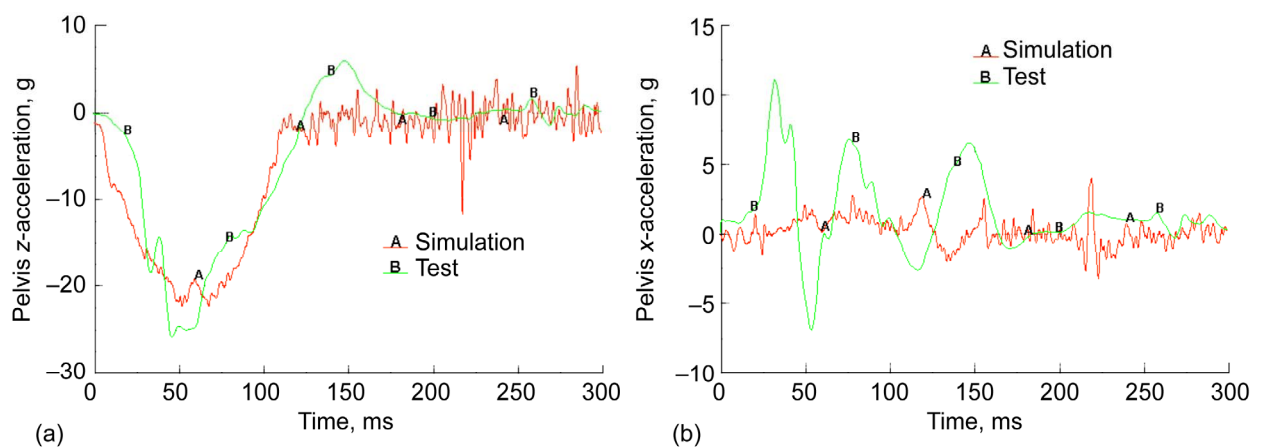

Figure 20.—Pelvis acceleration from Hybrid III physical and finite element dummies. (a) *z*-acceleration. (b) *x*-acceleration.
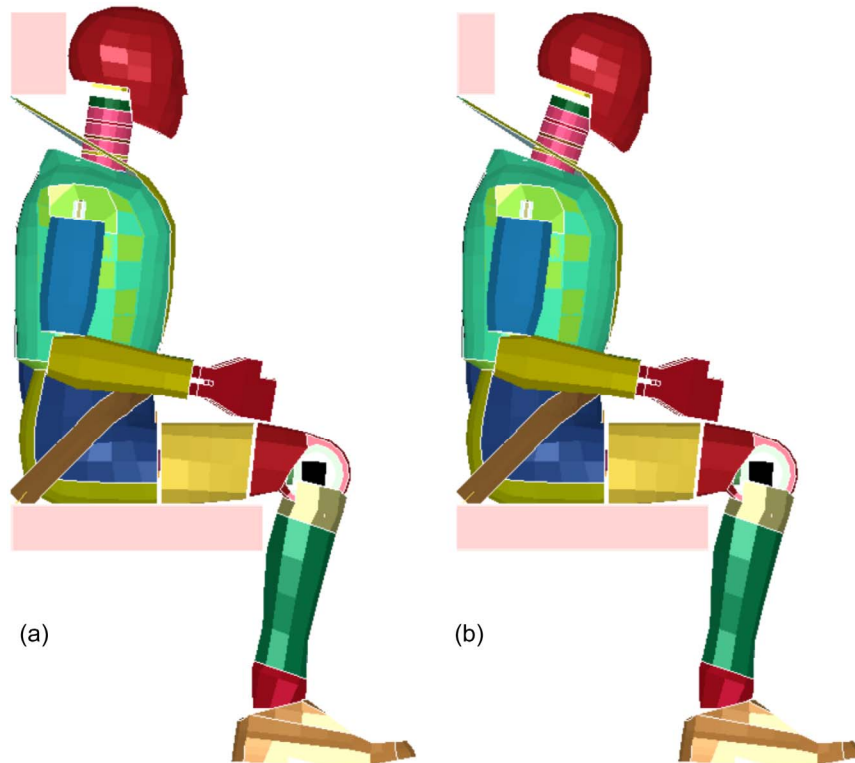
Figure 21.—Two different Hybrid III positions (different head pad thicknesses) at time zero for a simulation with a 20g impulse in the *z*-direction. (a) Position 1. (b) Position 2.
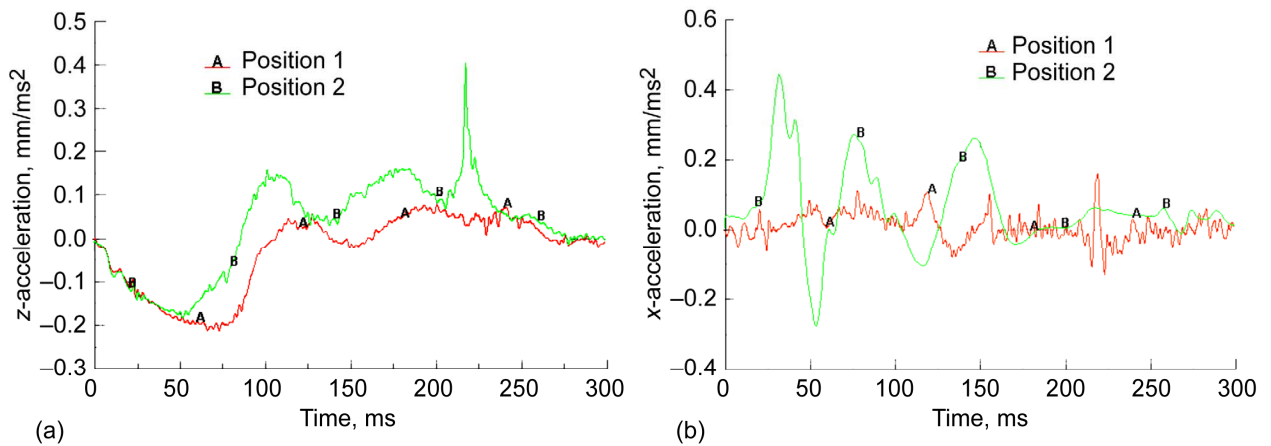

Figure 22.—Head acceleration for the two positions considered for the Hybrid III dummy (see Fig. 21).

Injury Assessment for a 10g Impulse in the Positive *x*-Direction

The experimental data from the tests can be used to determine the probability of injuries in a similar impact event. The injury criteria listed in the "Review of Human Injury Tolerance Criteria" section were used to determine the injury values. Table V summarizes the critical data with respect to some of the injury criteria listed in the previous section.

TABLE V.—INJURY ASSESSMENT AND CRITICAL INJURY VALUES

Criterion	Allowable	Predicted by test	Predicted by simulation	Pass or fail
Head Injury Criterion (HIC)	700	(a)	129.8	Pass
Chest severity index (CSI)	700	(a)	28.7	Pass
Thorax acceleration, g	60	27	10	Pass
Pelvis acceleration, g	130	12	15	Pass
Lumbar force, N	6672	1350	1250	Pass
Neck force, N	6806	(a)	3950	Pass
Neck moment flexion, N-m	310	14	8	Pass
Neck moment extension, N-m	135	7	14.5	Pass

[a]Not available.

Concluding Remarks

NASA undertook an experimental effort to determine crew response during landing of the *Orion* vehicle for a variety of landing orientations and velocities and crew protection systems. This effort consisted of testing Hybrid III test dummies under different loading impulses in different directions. Finite element (FE) models of the test setup were developed with the Hybrid III 50-percent rigid-deformable dummy. The models were validated by comparing results from the tests with computed results obtained by analyzing the FE dummy with the computational tool LS–DYNA. Kinematics data from the tests were compared with the predictions of the FE models. In addition, forces and moments in various parts of the test dummy were collected and compared with the prediction of the corresponding parts in the FE dummy. In general, good predictions were obtained by the FE dummy. However, better predictions could be obtained if the test setup of the test dummy better matched the positions of the FE dummy before testing.

In addition to validating the FE model with the test data, this paper presents several injury criteria. These criteria are widely used in the automotive industry and may be applicable to *Orion* if additional work is done to tailor the criteria to meet the safety requirements for the *Orion* program. These injury criteria were used to determine a potential-for-injury value by comparing the allowable injury criteria values with the values produced by tests and FE simulations.

References

Alem, Nabih M.; and Strawn, Gregory D. (1996): Evaluation of an Energy Absorbing Truck Seat for Increased Protection From Landmine Blasts. USAARL Report no. 96–06.

Armenia-Cope, R., et al. (1993): An Assessment of the Potential for Neck Injury Due to Padding of Aircraft Interior Walls for Head Impact Protection. DOT/FAA/AM–93/14.

Bostroem, Ola.; Svennsson, Mats; and Muser, Markus (1998): NIC Measurement Techniques and Result Interpretation. Presented at the NIC Meeting, Gothenburg, Sweden.

Brinkley, James W.; Specker, Lawrence J.; and Mosher, Stephen E. (1989): Development of Acceleration Exposure Limits for Advanced Escape Systems. AGARD CP–472.

Croft, A.C., et al. (2002): The Neck Injury Criterion: Future Considerations. Accid. Anal. Prev., vol. 34, no. 2, pp. 247–255.

Desjardins, S.P., et al. (1989): Aircraft Crash Survival Design Guide. USAAVSCOM TR–89–D–22D.

Fox, Roy G. (1988): OH–58 Energy Attenuating Crew Seat Feasibility Study. BHTI Report 699–099–286.

Gadd, Charles W. (1966): Use of a Weighted-Impulse Criterion for Estimating Injury Hazard. Proceedings of the 10th Stapp Car Crash Conference, Society of Automotive Engineers, New York, NY.

Gowdy, Van (1990): Development of a Crashworthy Seat for Commuter Aircraft. DOT/FAA/AM–90/11.

Haley, Joseph L., Jr.; and Palmer, Ronald W. (1994): Evaluation of a Retrofit OH–58 Pilot's Seat To Prevent Back Injury. USAARL Report No. 95–9.

Kecman, D. (1997): An Engineering Approach to Crashworthiness of Thin-Walled Beams and Joints in Vehicle Structures. Thin-Walled Struct., vol. 28, nos. 3/4, pp. 309–320.

Kellas, Sotiris; and Jones, Lisa E. (2002): Energy Absorbing Seat System for an Agricultural Aircraft. NASA/CR—2002-212132. http://ntrs.nasa.gov

Kleinberger, Michael, et al. (1999): Effects of Head Restraint Position on Neck Injury in Rear Impact. Presented at the Traffic Safety and Auto Engineering Stream of the Whiplash-Associated Disorders World Congress, Vancouver, Canada.

Laananen, David H. (1993): Crashworthiness Analysis of Commuter Aircraft Seats. DOT/FAA/CT–TN91/28.

Lau, Ian V.; and Viano, David C. (1986): The Viscous Criterion—Bases and Applications of an Injury Severity Index for Soft Tissues. Proceedings of the 30th Stapp Car Crash Conference, SAE Paper 861882, Society of Automotive Engineers, Warrendale, PA, pp. 123–142.

LS–DYNA Keyword User's Manual (2007) Version 971, Livermore Software Technology Corporation (LSTC).

McHenry, Brian G. (2004): Head Injury Criterion and the ATB. http://www.mchenrysoftware.com/ HIC and the ATB.pdf

Mertz, H.J.; and Gadd, C.W. (1971): Thoracic Tolerance to Whole-Body Deceleration. Proceedings of the 15th Stapp Car Crash Conference, SAE Paper 710852, Society of Automotive Engineers, New York, NY, pp. 135–152.

Mertz, H.J.; and Patrick, L.M. (1971): Strength and Response of the Human Neck. Proceedings of the 15th Stapp Car Crash Conference, SAE Paper 710855, Society of Automotive Engineers, New York, NY, pp. 207–255.

Nirula, R., et al. (2003): Correlation of Head Injury to Vehicle Contact Points Using Crash Injury Research and Engineering Network Data. Accid. Anal. Prev., vol. 35, no. 2, pp. 201–210.

Nusholtz, G.S., et al. (2003): Studies of Neck Injury Criteria Based on Existing Biomechanical Test Data. Accid. Anal. Prev., vol. 35, no. 5, pp. 777–786.

Schmitt, Kai-Uwe; Niederer, Peter F.; and Walz, Felix H. (2004): Trauma Biomechanics: Introduction to Accidental Injury. Springer, Berlin.

Tabiei, Ala; and Nilakantan, Gaurav (2007): Reduction of Crew Injury Caused by Acceleration From Mine Blast/ IED, 6th European LS–DYNA Users' Conference, Gothenburg, Sweden.

Teng, Tso-Liang, et al. (2004): The Study of Head and Neck Injury in Traffic Accidents. J. Appl. Sci., vol. 4, no. 3, pp. 449–455.

Tyrell, D.; and Severson, K. (1996): Crashworthiness Testing of Amtrak's Traditional Coach Set, Safety of High-Speed Ground Transportation Systems. DOT/FRA/ORD–96/08.

Welcher, Judson B.; and Szabo, Thomas J. (2001): Relationships Between Seat Properties and Human Subject Kinematics in Rear Impact Tests. Accid. Anal. Prev., vol. 33, no. 3, pp. 289–304.

REPORT DOCUMENTATION PAGE

1. REPORT DATE *(DD-MM-YYYY)* 01-03-2009	2. REPORT TYPE Technical Memorandum	3. DATES COVERED *(From - To)*

4. TITLE AND SUBTITLE
Validation of Finite Element Crash Test Dummy Models for Predicting *Orion* Crew Member Injuries During a Simulated Vehicle Landing

5a. CONTRACT NUMBER

5b. GRANT NUMBER

5c. PROGRAM ELEMENT NUMBER

6. AUTHOR(S)
Tabiei, Al; Lawrence, Charles; Fasanella, Edwin, L.

5d. PROJECT NUMBER

5e. TASK NUMBER

5f. WORK UNIT NUMBER
WBS 510505.05.03.07.13

7. PERFORMING ORGANIZATION NAME(S) AND ADDRESS(ES)
National Aeronautics and Space Administration
John H. Glenn Research Center at Lewis Field
Cleveland, Ohio 44135-3191

8. PERFORMING ORGANIZATION REPORT NUMBER
E-16677

9. SPONSORING/MONITORING AGENCY NAME(S) AND ADDRESS(ES)
National Aeronautics and Space Administration
Washington, DC 20546-0001

10. SPONSORING/MONITORS ACRONYM(S)
NASA

11. SPONSORING/MONITORING REPORT NUMBER
NASA/TM-2009-215476

12. DISTRIBUTION/AVAILABILITY STATEMENT
Unclassified-Unlimited
Subject Category: 18
Available electronically at http://gltrs.grc.nasa.gov
This publication is available from the NASA Center for AeroSpace Information, 301-621-0390

13. SUPPLEMENTARY NOTES

14. ABSTRACT
A series of crash tests were conducted with dummies during simulated Orion crew module landings at the Wright-Patterson Air Force Base. These tests consisted of several crew configurations with and without astronaut suits. Some test results were collected and are presented. In addition, finite element models of the tests were developed and are presented. The finite element models were validated using the experimental data, and the test responses were compared with the computed results. Occupant crash data, such as forces, moments, and accelerations, were collected from the simulations and compared with injury criteria to assess occupant survivability and injury. Some of the injury criteria published in the literature is summarized for completeness. These criteria were used to determine potential injury during crew impact events.

15. SUBJECT TERMS
Spacecraft design; Landing; Astronauts; Risk

16. SECURITY CLASSIFICATION OF:			17. LIMITATION OF ABSTRACT	18. NUMBER OF PAGES	19a. NAME OF RESPONSIBLE PERSON STI Help Desk (email:help@sti.nasa.gov)
a. REPORT U	b. ABSTRACT U	c. THIS PAGE U	UU	30	19b. TELEPHONE NUMBER *(include area code)* 301-621-0390